Research Article

Nano Research
2022, 15(7): 6306–6314

ISSN 1998-0124 CN 11-5974/O4
https://doi.org/10.1007/s12274-022-4254-1

A targeted nanoplatform co-delivery of pooled siRNA and doxorubicin for reversing of multidrug resistance in breast cancer

Hongmei Liu[1,2,§], Ding Ma[3,§], Jinpeng Chen[4,§], Li Ye[2], Yiping Li[5], Yuexia Xie[2], Xue Zhao[2], Hanbing Zou[2], Xiaojing Chen[2], Jun Pu[1], and Peifeng Liu[1,2] (✉)

[1] *State Key Laboratory of Oncogenes and Related Genes, Shanghai Cancer Institute, Renji Hospital, Shanghai Jiao Tong University School of Medicine, Shanghai 200032, China*
[2] *Central Laboratory, Renji Hospital, School of Medicine, Shanghai Jiao Tong University, Shanghai 200127, China*
[3] *Department of Biliary-Pancreatic Surgery, Shanghai Jiao Tong University School of Medicine Affiliated Renji Hospital, Shanghai 200127, China*
[4] *Thyroid Breast Surgery, Nantong First People's Hospital, Nantong 226001, China*
[5] *Shanghai University of Traditional Chinese Medicine, Shanghai 200032, China*
[§] *Hongmei Liu, Ding Ma, and Jinpeng Chen contributed equally to this work.*

Received: 6 December 2021 / **Revised:** 17 February 2022 / **Accepted:** 20 February 2022

ABSTRACT

Multi-drug resistance (MDR) has become the largest obstacle to the success of cancer patients receiving traditional chemotherapeutics or novel targeted drugs. Here, we developed a targeted nanoplatform based on biodegradable boronic acid modified ε-polylysine to co-deliver P-gp siRNA, Bcl-2 siRNA, and doxorubicin for overcoming the challenge. The targeted nanoplatform showed a robust suppressing efficiency for the invasion, proliferation, and colony formation of adriamycin (ADR) resistant breast cancer cell line (MCF-7/ADR) cells *in vitro*. The ATP responsiveness of the nanoplatform was also proved in the research. In the *in vivo* antitumor experiment, the targeted nanoplatform showed a significant inhibition of tumor growth with good biocompatibility. The goal of this study is to develop a novel and facile strategy to prepare a highly efficient and safe gene and drug delivery system for MDR breast cancer based on biocompatible ε-polylysine polymers.

KEYWORDS

multi-drug resistance (MDR), breast cancer, adenosine triphosphate (ATP) responsiveness, ε-polylysine

1 Introduction

Breast cancer is one of the most common malignant tumors in women, and its incidence has been increasing year by year [1, 2]. Fortunately, breast cancer is one of the solid tumors that are sensitive to chemotherapy [3, 4]. Chemotherapy plays an irreplaceable role in the comprehensive treatment of breast cancer [4–8]. Multidrug resistance (MDR) in cancer is the main reason for this phenomenon [9–11]. Anticancer drugs encapsulated in nanoparticles can actively or passively target tumor cells and thus improve the therapeutic effect at the target site. This can reduce the systemic toxicity of chemotherapy drugs and bypass certain forms of multidrug resistance to some extent [12].

Clinically, the reasons of MDR to cancer cells are multiple, such as overexpression of the adenosine triphosphate-binding cassette (ABC) transmembrane transporter protein P-glycoprotein (MDR1/P-gp), gene mutation, epithelial-mesenchymal transition (EMT), modification of the cell cycle, and inhibition of cell apoptosis [13]. Overexpression of P-glycoprotein (MDR1/P-gp) and inhibition of cell apoptosis are main reasons of MDR in breast cancer [10, 13]. So far, siRNAs have been widely investigated to knockdown the expression of MDR-related proteins (siP-gp) and to knockdown anti-apoptotic protein such as Bcl-2 (siBcl-2) that can inhibit cell apoptosis in MDR breast cancer cells [14–16].

Efficient RNA interference actually requires suitable RNA carriers [17–21]. Cationic polymers with nucleic acid-binding moieties are easy-to-manufacture and widely used as promising gene vectors to introduce exogenous nucleic acid into targeted cells [22, 23]. However, cationic polymer-based gene vectors are associated with the "malignant" correlation between transfection efficacy and cytotoxicity [24]. Polymers with high molecular weight have high transfection efficacy but devastating toxicity [19, 25, 26]. If we can improve the transfection efficiency of cationic polymers without safety concerns, it would be very meaningful.

As one kind of poly-L-lysine (PLL) polymers, ε-polylysine is produced by microbial synthesis as naturally occurring polymers and is widely used in various food, medicinal, and electronics products with negligible safety concerns [27, 28]. ε-polylysine (ε-PLL) has an overall positive charge due to its many ε-amine groups and can compact or condense plasmid DNA into complexes [29–33]. However, the performances of ε-polylysine as well as current polymer-based products in gene transfection are less than ideal.

Phenylboronic acid (PBA) is a biocompatible group and capable of forming reversible covalent esters with 1,2- or 1,3-cis-diols on a ribose ring [34–37]. Therefore, PBA has been used as a targeting ligand to target cell overexpressing sialic acid. Besides, PBA has also been used in gene delivery systems. Cheng' group

Address correspondence to liupeifeng@yahoo.com

functionalized cationic dendrimers with PBA for efficient DNA, siRNA and protein delivery and polyethylenimine's gene delivery efficacy was also improved after PBA modification [22, 38–40].

To verify that the interaction of boronic acid with ε-polylysine played a role in the ε-polylysine based gene delivery system, we modified PBA to ε-polylysine to co-deliver siRNA and drug for the treatment of MDR breast cancer. siP-gp and siBcl-2 were selected to reverse the multidrug resistance breast cancer MCF-7/adriamycin (ADR) cells (Scheme 1). The gene silencing efficiency and drug killing power of MDR breast cancer *in vitro* and *in vivo* were intensively investigated. The goal of this study is to develop a novel and facile strategy to prepare a highly efficient and safe gene and drug delivery system for MDR breast cancer based on biocompatible and ε-polylysine polymers.

2 Experimental section

2.1 Materials

ε-PLL (molecular weight: 4,224 Da; number of surface amine groups: 33), were purchased from Macklin (Shanghai, China). 4-(Bromomethyl) phenylboronic acid, doxorubicin (DOX), and adenosine triphosphate (ATP) were purchased from Sigma-Aldrich (St. Louis, MO, USA). Hyaluronic acid (HA, molecular weight: 10 kDa) was purchased from Dalian Meilun Biotechnology Co., Ltd. (Dalian, China). Triethylamine (TEA), diethyl ether and methanol were purchased from Sinopharm Chemical Reagent Co., Ltd. (Shanghai, China). All siRNAs including fluorescently labeled siRNA (with a FAM conjugated at the 5' end of siRNA, siRNA-FAM) and scrambled siRNA non-specific to any human gene (siNC) were synthesized by GenePharma Co., Ltd. (Shanghai, China). The sequences for the sense and antisense strands of siRNAs are as follows: siP-gp (targeting P-glycoprotein), sense: 5'-CCCUAUUCUCCUUCUUCGCdTdT-3'; antisense: 5'-GCGAAGAAGGAGAAUAGGGdTdT-3'; siBcl-2 (targeting Bcl-2), sense: 5'-CCGGGAGAUAGUGAUGAAGdTdT-3'; antisense: 5'-CUUCAUCACUAUCUCCCGGdTdT-3'; siNC (non-specific to any human gene), sense: 5'-UCACGUUGAUAACCCAA AUdTdT-3'; antisense: 5'-AUUUGGGUUAUCAACGUGAdT dT-3'.

2.2 Synthesis and characterization of ε-PLL-PBA

100 mg ε-PLL dissolved in dehydrated methanol was added dropwise into the 4-(bromomethyl) phenylboronic acid solution (the molar ratios of PBA to ε-PLL were 8 and 16, respectively) followed by addition of TEA. The mixtures were stirred at 50 °C for 48 h.

After 48 h, the reaction solution was precipitated in diethyl ether three times. Finally, the yielding products were lyophilized. The materials were characterized by ^{1}H NMR spectroscopy (Varian, 699.804 MHz).

2.3 Cellular uptake of the fluorescently labeled polyplexes

ADR resistant breast cancer cells (MCF-7/ADR) were cultured in 24-well plates. Polyplexes consisted of PBA modified ε-PLL and siRNA-FAM were prepared at N/P ratios of 1:1, 2:1, 4:1, 8:1 and 10:1, respectively, with 20 pmol siRNA-FAM. N here represents the number of residual primary amine groups on the surface of

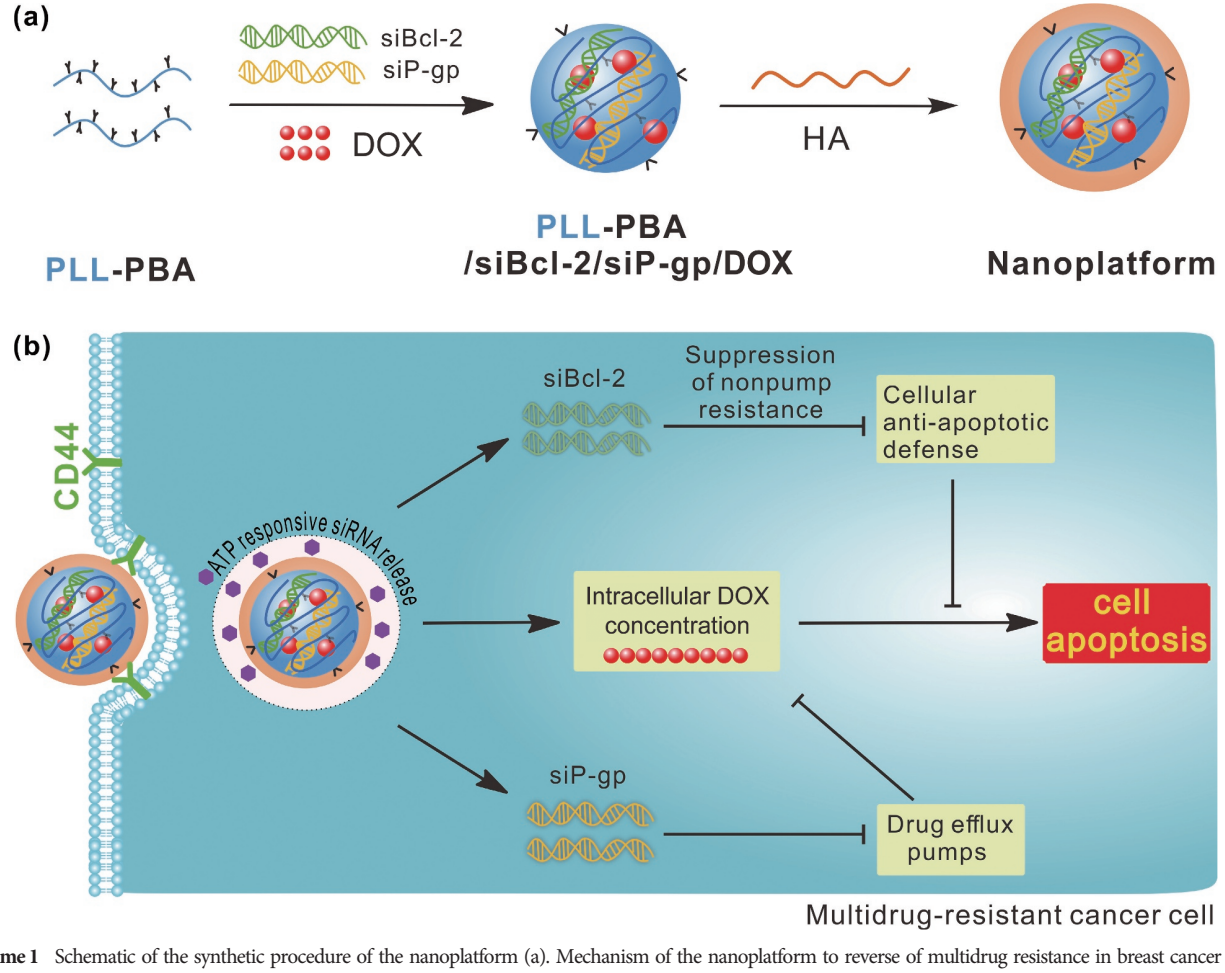

Scheme 1 Schematic of the synthetic procedure of the nanoplatform (a). Mechanism of the nanoplatform to reverse of multidrug resistance in breast cancer MCF-7/ADR cells (b).

PBA modified ε-PLL; P here represents the number of phosphate anions in the siRNA chains. The polyplexes were incubated for 30 min before addition into the wells. After incubation for 6 h, the fluorescence of FAM in the transfected cells was observed by a fluorescent microscopy (Leica, Germany).

For preparation of ε-PLL-PBA-siRNA-DOX-HA polyplex, ε-PLL-PBA, siRNA and DOX were mixed and incubated for 30 min. After that, HA was added to the mixture and incubated for another 30 min with different mass ratios of ε-PLL-PBA to HA. The fluorescence of DOX in the transfected cells was observed by a fluorescent microscopy (Leica, Germany).

2.4 Characterization of the polyplexes

The sizes of the polyplexes at optimized conditions were measured by dynamic light scattering (DLS) using a Malvern Zetasizer (Nano ZS 90, Malvern, UK) at 25 °C. The morphology of the polyplexes was further characterized by a transmission electron microscope (TEM, HT7700, HITACHI, Japan).

2.5 Cell culture and treatment

The human breast cancer cell line MCF-7 was purchased from the Cell Bank of the Chinese Academy of Sciences (Shanghai, China), and cultured in Dulbecco's modified Eagle medium (DMEM) supplemented with 10% fetal bovine serum at 37 °C and 5% CO_2. DOX-resistant breast cancer cell line MCF-7/ADR was purchased from Shanghai Aulu Biological Technology (Shanghai, China) and cultured in DMEM with 10% fetal bovine serum and 1,000 ng/mL DOX at 37 °C and 5% CO_2.

2.6 Gel retardation assay

After fully incubating 5 μL of the complex with 1 μg siRNA, 1 μL of 6× loading buffer (Takara Biotechnology, Dalian, China) was added to the suspensions, and then added into a 1% agarose gel with 5 μg/mL gel-green. The loaded agarose gel was run by electrophoresis in 1× Trisacetate-ethylene diamine tetraacetic acid (EDTA) (TAE) running buffer at 90 V for 15 min. Lastly, the siRNA image was recorded on an image master VDS thermal imaging system (Bio-Rad, CA, USA) under the ultraviolet wavelength of 254 nm.

2.7 q-PCR

According to the manufacturer's instruction (Ambion, Life Technologies), TRIzol was used to extract total RNA from the treated cells. After measuring the RNA concentrations by a Nanodrop 2000 spectrophotometer, the Prime Script RT Reagent Kit with gDNA Eraser was used to reverse 1.0 μg RNA of each sample according to the manufacturer's instructions (TaKaRa). Quantitative polymerase chain reaction (q-PCR) was performed using TB Green Premix Ex Taq II according to the manufacturer's instructions (TaKaRa). The ΔΔCt method was used to calculate relative gene expression, while GAPDH was used as the internal control. The primers used in the PCR reactions were as follow: DAPDH: 5'- ACA ACT TTG GTA TCG TGG AAGG-3' and 5'- GCC ATC ACG CCA CAG TTTC-3'; Bcl-2: 5'-GGT GGG GTC ATG TGT GTG-3' and 5'- CGG TTC AGG TAC TCA GTC ATCC-3'; P-gp: 5'- GGG ATG GTC AGT GTT GAT GGA-3' and 5'- GCT ATC GTG GTG GCA AAC AATA-3'.

2.8 Cytotoxicity and cell proliferation assay

The cytotoxicity of the complex and cell proliferation assay was performed by Cell Counting Kit-8 (CCK-8). For cytotoxicity assay, 5×10^3 cells were seeded in 96-well plates, then treated with each group for 24, 48 and 72 h. For cell proliferation assay, 1×10^3 cells were seeded in 96-well plates and treated with each group for 24 h. After that, 10 μL of CCK-8 solution was added to each well and incubated for 1 h. Lastly, the absorbance was measured at 450 nm.

2.9 Colony formation assay

For this assay, 1×10^3 cells were seeded in 6-well plates and cultured at 37 °C and 5% CO_2 for about 14 days. Once the colonies of cancer cell could be visually observed, the cells were treated with 10% methanol and then treated with crystal violet for 30 min.

2.10 Transwell invasion assay

For this assay, 1×10^5 cancer cells were resuspended in serum-free medium and added to upper chambers of Corning BioCoat Matrigel invasion chambers (8 μm, 24-well format; Corning, Lowell, MA, USA). Then, the lower chambers of 24-well plates were added 0.6 ml of medium with 10% FBS. After culturing at 37 °C and 5% CO_2 for 24 h, the upper chambers were treated with 10% methanol and then treated with crystal violet for 30 min. Finally, counted the cells in the lower member of the upper chamber carefully by inverted microscope.

2.11 Wound healing assay

In 6-well plates, cancer cells were cultured to confluence. The monolayer of cancer cells was scraped with A 200 μL pipette tip to form three separate wounds, and then treated with different conditions. After 0, 12 or 24 h, an inverted microscope was used to photograph the plates and carefully measured the gaps between edges of wounds.

2.12 *In vivo* polyplexes treatment

Four-week-old female BALB/c nude mice were used to establish orthotopic breast cancer xenografts. All experimental animals were purchased from the Institute of Zoology, Chinese Academy of Sciences of Shanghai. The animal experiments were approved by the Ethics Committee of Renji Hospital, Shanghai Jiao Tong University School of Medicine. Briefly, 2×10^6 cancer cells were injected into the left thoracic mammary fat pad of female nude mice. One week later, complexes were injected through tail vein 3 times a week. All mice were divided into 5 groups, including ε-PLL-PBA-siRNA-DOX-HA (HA/BP-DOX group), complexes loaded with negative control RNA (ε-PLL-PBA-NC-DOX-HA, HA/NC-DOX group), no HA complexes (ε-PLL-PBA-siRNA-DOX, BP-DOX group), DOX treatment alone (DOX group), and saline controlled group (control group). For each treatment, 10 nmol siRNA (5nmol siP-gp and 5 nmol siBcl-2) and 40 μg DOX (2 mg/kg) were injected to each mouse. The body weight of each mouse and the length and width of each tumor were measured every 7 days. The tumor volume was calculated using the formula: tumor volume = (width^2 × length)/2. Inhibition rate (%) = 100 – (mean of final tumor volumes of treatment group – mean of initial tumor volumes of treatment group)/(mean of final tumor volumes of control group – mean of initial tumor volumes of control group) × 100. Mouse were sacrificed by cervical decapitation after 5 weeks treatment. Major organs and xenograft tumor tissues of mouse were fixed for hematoxylin-eosin (HE) staining. The tumor tissues were also stained with P-gp and Bcl-2 immunohistochemistry. In all *in vivo* experiments, 5 mice were used in each group.

2.13 Immunohistochemistry

Immunohistochemistry stainings were performed according to the manufacturer's instructions of LSAB+ kit (Dako, USA). Rabbit anti-P-gp and anti-Bcl-2 antibody (1:500, Abcam) were used to perform immunohistochemistry stains.

2.14 Statistical analyses

SPSS 13.0 software was used for statistical analyzes. For comparison among groups, analysis of variance (ANOVA) and Student's *t*-test were used. The chi-square test was used for the comparison of categorical data. A p-value less than 0.05 was considered statistically significant.

3 Results and discussion

3.1 Synthesis and characterization of the PBA modified ε-PLL polymers

PBA-modified ε-PLL polymers were synthesized using a facile strategy, as shown in Fig. 1(a). The average number of PBA moieties conjugated to each ε-PLL polymer was calculated using ^{1}H nuclear magnetic resonance (NMR) analysis. Both the proton peaks for PBA and ε-PLL are observed in the spectra (Fig. S1 in the Electronic Supplementary Material (ESM)). According to the integrated peak areas, the average number of PBA modified on each ε-PLL was calculated to be 7 and 9, and the obtained products are defined as PLL-PBA7 and PLL-PBA9, respectively. In order to obtain targeted nanoparticles, catechol (Cat) modified hyaluronic acid (HA-Cat) was synthesized by reacting HA with dopamine, as illustrated in Fig. 1(b). ^{1}H NMR (Fig. S1 in the ESM) confirmed the successful modification of dopamine.

3.2 Synthesis and characterization of HA modified complexes

The fluorescently labeled siRNA was used to evaluate cellular uptake efficiencies of siRNA delivered by PLL-PBA7 and PLL-PBA9 with N/P ratios of 1:1, 2:1, 4:1, 6:1, 8:1 and 10:1. We found that the strongest fluorescence of siRNA-FAM was showed in the cytoplasm of ADR resistant breast cancer cells (MCF-7/ADR) treated with PLL-PBA9/siRNA complexes (N/P = 2:1) (Fig. S2 in the ESM). Thus, in the following experiment, we chose this optimized ratio to conduct the following experiments.

PLL-PBA9/siRNA/DOX complexes were formed by mixing PLL-PBA9, siRNA and DOX. HA-Cat was shielded on the surface of PLL-PBA9/siRNA/DOX complexes to form HA/PLL-PBA9/siRNA/DOX complexes through charge interactions and benzenediol groups in HA-Cat and PBA groups in PLL-PBA. We observed the fluorescence intensity of DOX in PLL-

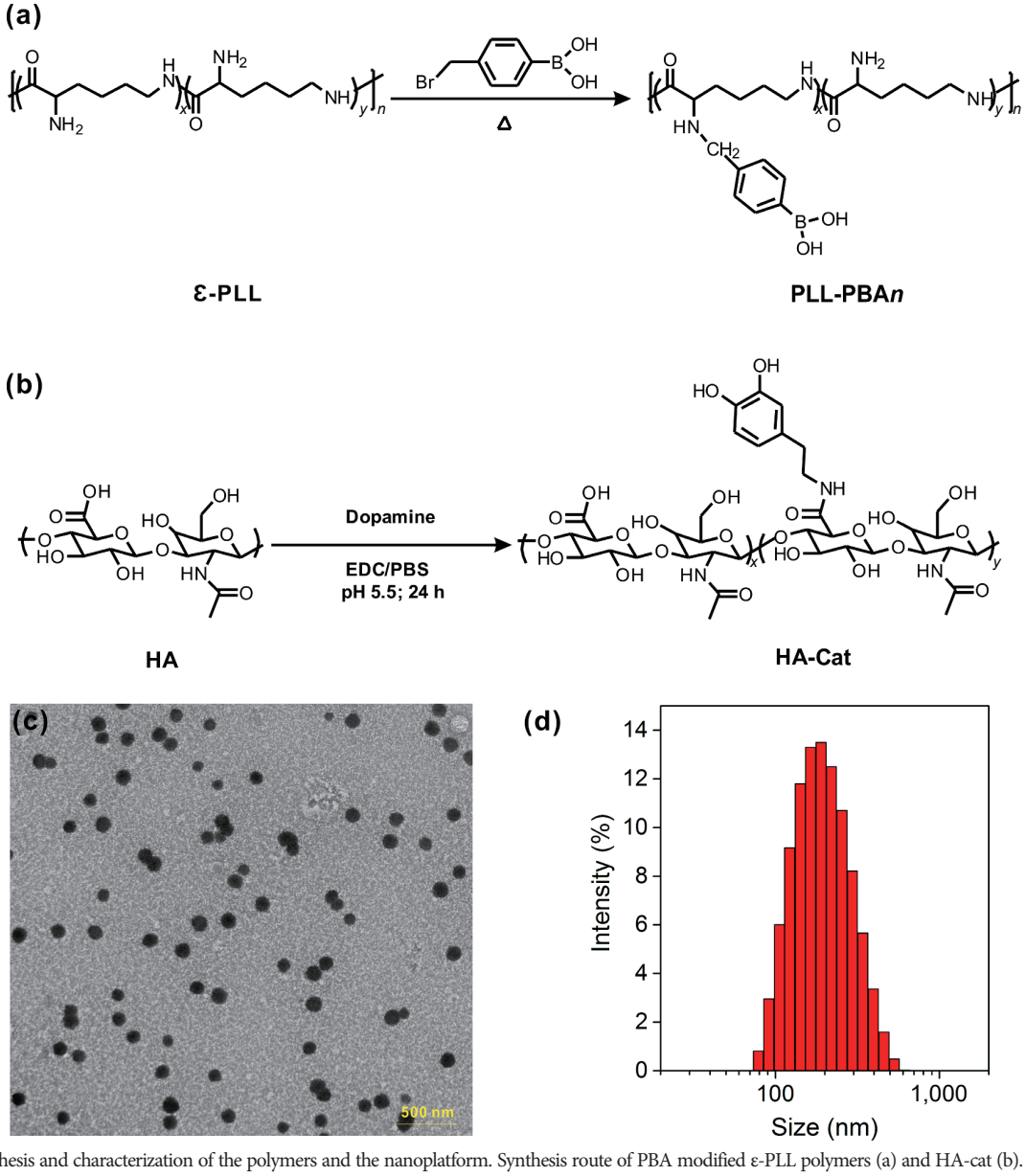

Figure 1 Synthesis and characterization of the polymers and the nanoplatform. Synthesis route of PBA modified ε-PLL polymers (a) and HA-cat (b). TEM image (c) and hydrodynamic size (d) of the HA coated nanoplatform.

PBA9/siRNA/DOX complexes with mass ratio range of PLL-PBA9 to HA from 1:0.5 to 1:3. When the mass ratio of PLL-PBA9 to HA was 1:1, the cellular uptake efficiencies for DOX in MCF-7/ADR human breast cancer cells were extremely strongest (Fig. S3 in the ESM). Therefore, molar ratio of PLL-PBA9 to HA equal to 1:1 was selected to form the HA coated nanoplatform (HA/PLL-PBA9/siRNA/DOX).

It is well known that polyplexes with a size around 200 nm are suitable for gene transfection. We measured the sizes and the morphology of the polyplexes at optimized conditions by TEM (HT7700, HITACHI, Japan) and DLS (Figs. 1(c) and 1(d)). The hydrodynamic sizes of HA/PLL-PBA9/siRNA/DOX complexes were measured to be around 180.2 nm (Fig. 1(d)).

Efficient and rapid release of siRNA in the cytoplasm is essential but a challenging issue for siRNA drug development. As mentioned before, phenylboronic acid is capable of forming reversible covalent esters with 1,2- or 1,3-cis-diols on a ribose ring, a structure which is present at the 3' end of RNAs, several kinds of ribonucleotides and ATP. ATP is present in the extracellular environment at about 0.4 mM but is dramatically higher (up to 3–5 mM) within the intracellular matrix [41, 42]. In accordance with Fig. S4 in the ESM, the complex stability (that is resistance to ATP) strikingly depends on the concentration of ATP. When the concentration of ATP reached about 5 mM, siRNA was released form the complexes. In conclusion, this targeted nanoplatform can achieve ATP concentration-dependent siRNA release.

3.3 *In vitro* effect of the polyplexes

siP-gp (targeting P-glycoprotein) and siBcl-2 (targeting anti-apoptotic protein Bcl-2) were encapsulated in the HA/siP-gp-PLL-PBA9-siBcl-2 complexes (HA/BP) to reverse multidrug resistance of the MCF-7/ADR human breast cancer cells. The HA/siP-gp-PLL-PBA9 complexes (HA-P) only encapsulating siP-gp and the HA/PLL-PBA9-siBcl-2 complexes (HA-B) only encapsulating siBcl-2 were selected as controls.

As shown in Fig. 2(a), both HA/BP and HA/P complexes efficiently induced P-gp gene knockdown on the MCF-7/ADR human breast cancer cells (relative P-gp gene level: HA/BP vs. HA/P: 0.4864 ± 0.0264 vs. 0.6338 ± 0.0709). The P-gp gene expression were not induced in the groups of HA/B and the groups with siNC loading (HA/NC). Bcl-2 gene expression was the same with that of P-gp gene. Down-regulation of Bcl-2 gene expression in MCF-7/ADR human breast cancer cells (Fig. 2(b)) was also showed by both HA/BP and HA/B complexes (relative Bcl-2 gene level: HA/BP vs. HA/B: 0.2769 ± 0.0301 vs. 0.3342 ± 0.0458). Silencing the expression of MDR-related proteins (siP-gp) and anti-apoptotic protein such as Bcl-2 (siBcl-2) in MCF-7/ADR cells would restore drug sensitivity to MCF-7/ADR cells. Therefore, HA/siP-gp-PLL-PBA9-siBcl-2-DOX complexes (HA/BP-DOX) effectively killed MCF-7/ADR cells (Fig. 2(c)). In the contrast, the complexes HA/NC-DOX with the same DOX concentration did not block MCF-7/ADR cells growth and even promoted cells growth (Fig. 2(c)). When loading only siP-gp or only siBcl-2, the complexes HA/P-DOX or HA/B-DOX also caused MCF-7/ADR cells death to a certain degree. We also investigated the vector PLL-PBA9 and HA exhibited negligible cytotoxicity against the MCF-7/ADR cells at tested concentrations after incubation of 24 h (Fig. 2(d)). The above experimental results proved that co-delivery of siP-gp and siBcl-2 by HA/PLL-PBA9 would reverse multidrug resistance of the MCF-7/ADR human breast cancer cells.

In addition to the treatment sensitivity of HA/BP complexes on MCF-7/ADR cells, we further investigated the effect of MCF-7/ADR complexes on cell invasion, migration, and colony formation. The abilities of cell invasion, proliferation, and colony formation were interrelated to cancer cell proliferation ability and metastasis [43, 44]. Invasion of carcinomas is defined as the penetration of tissue barriers and migration is often used to describe any directed cancer cell movement and the ability to move within tissues or between different organs, both of which

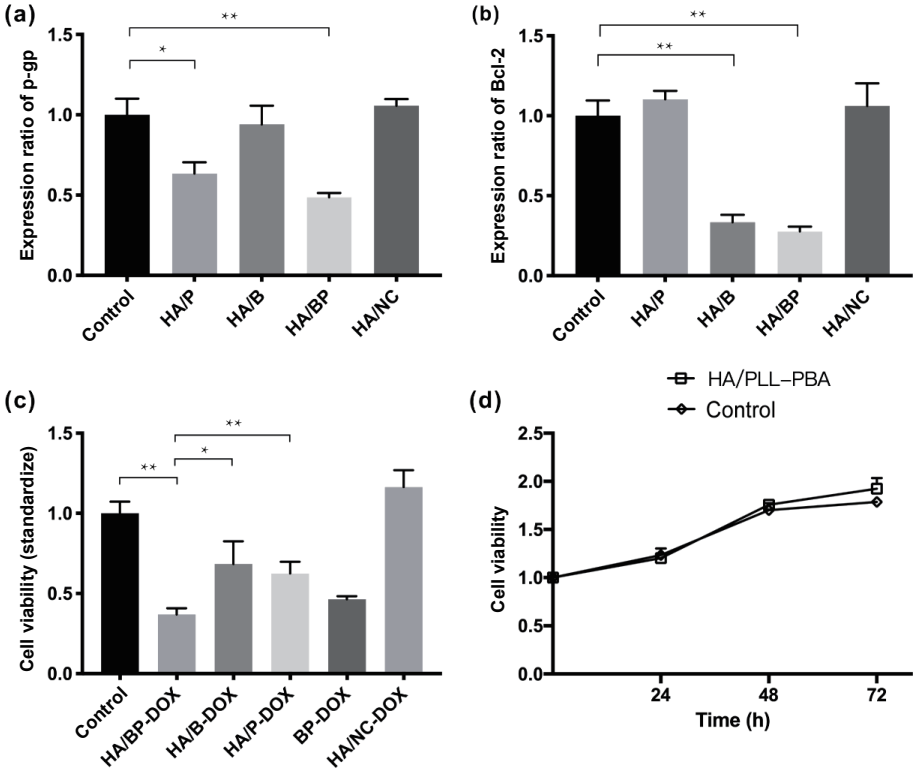

Figure 2 *In vitro* RNA transfection and cytotoxicity of complexes. Relative expression of p-gp (a) and Bcl-2 mRNA (b) in MCF-7/ADR human breast cancer cells. Cytotoxicity of the complexes (c) and HA/PLL-PBA (d). The siRNA concentration in all groups was 150 pmol/mL. The DOX concentration in all groups was 1,000 ng/mL. $^{*}P < 0.05$; $^{**}P < 0.01$.

would be responsible for tumor metastasis eventually. The result of cell invasion showed that HA/siP-gp-PLL-PBA9-siBcl-2-DOX complexes (HA/BP-DOX) exhibited a robust suppressing efficiency for the invasion of MCF-7/ADR cells (Fig. 3, HA/BP-DOX vs. control: 45.3 ± 10.4 vs. 496.7 ± 73.7, $P < 0.01$). The complexes with only siP-gp or siBcl-2 loading (HA/P-DOX and HA/B-DOX) also exhibited a moderate degree of suppressing efficiency for the invasion of MCF-7/ADR cells (HA/P-DOX vs. HA/B-DOX, 230.7 ± 10.1 vs. 200.0 ± 50.0). As expected, the complexes with siNC and DOX loading (HA/NC-DOX) had a low effect on the cell invasion (Fig. 3, HA/NC-DOX vs. control: 426.7 ± 46.9 vs. 496.7 ± 73.7, $P > 0.05$).

These results of cell colony formation were the same with that of cell invasion (Figs. 4(a) and 4(b)). HA/BP-DOX complexes showed the strongest suppressing effect on the formation ability of cell colony (HA/BP-DOX vs. control: 0.2900 ± 0.0656 vs. 0.7533 ± 0.1242, $P < 0.01$) and the complexes HA/P-Dox and HA/B-Dox also have suppressing effects on the formation ability of cell colony to some extent. Subsequently, the inhibition efficiency of the complexes on migration ability was also investigated and the strongest suppressing effect on cell migration ability was observed in the cells treated with HA/BP-DOX complexes (Fig. 5(a)). The effect of the complexes on cell migration ability was also quantitatively evaluated by wound healing assay. As shown in Fig. 5(b), HA/BP-DOX complexes significant extended the distance between wound edges in MCF-7/ADR cells (HA/BP-DOX vs. control: 66.97% vs. 25.19%, $P < 0.01$). Whereas the HA/NC-Dox proved useless in colony formation and would healing ability of MCF-7/ADR human breast cancer cells (HA/NC-DOX vs. control: 0.8167 ± 0.0929 vs. 0.7533 ± 0.1242, $P > 0.05$ for colony formation (Fig. 4) and 19.19% vs. 25.19%, $P > 0.05$ for would healing (Fig. 5)).

It is worth noting that the complexes with no HA coating on the wrapped also had great suppressing effects on cell invasion, proliferation, and colony formation (Figs. 3–5). This is mainly because BP-DOX complexes have the positive charge and can also achieve efficient siRNA delivery *in vitro*. To sum up, the nanoplatform (HA/siP-gp-PLL-PBA9-siBcl-2 complexes) reverses multidrug resistance in breast cancer MCF-7/ADR cells, kills the MCF-7/ADR cells efficiently, and inhibits the abilities of cancer cell migration, invasion and colony formation, which will lay a foundation for the treatment of breast cancer with multi-drug resistance (MDR) *in vivo*.

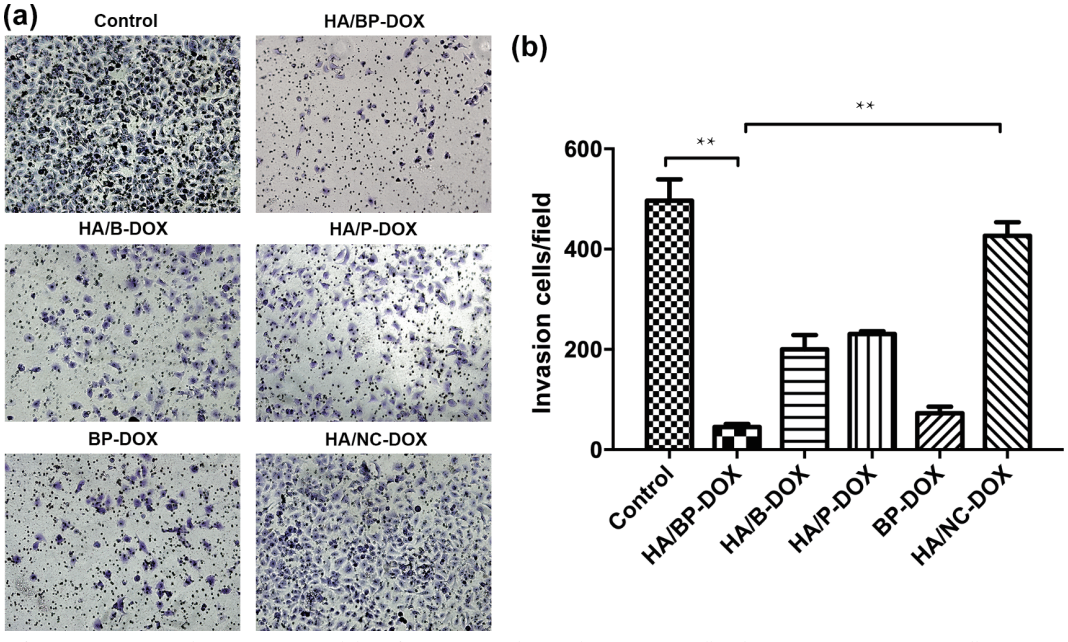

Figure 3 Effect of HA/BP-DOX complexes on invasion ability of MCF-7/ADR human breast cancer cells. The siRNA concentration in all groups was 150 pmol/mL. The DOX concentration in all groups was 1,000 ng/mL. *$P < 0.05$; **$P < 0.01$. Scale bars: 100 μm.

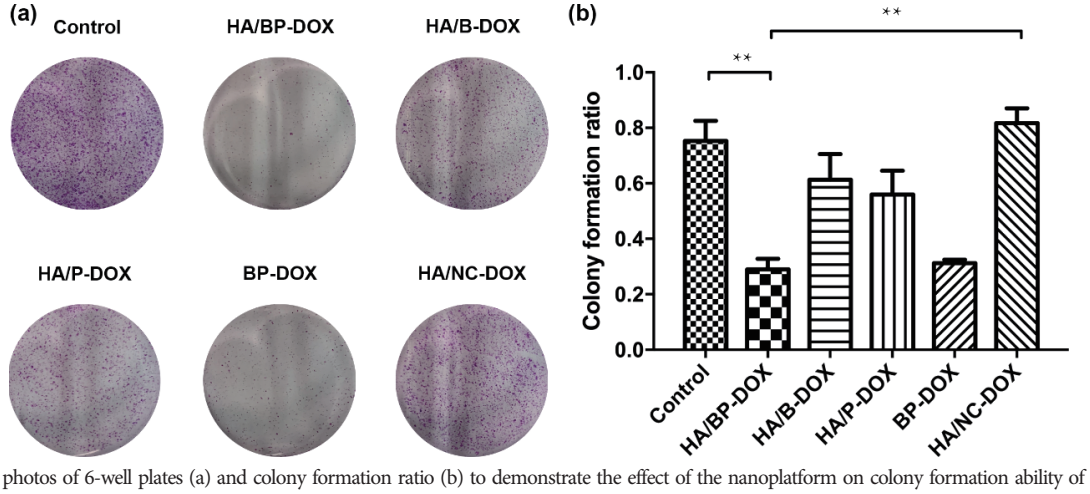

Figure 4 The photos of 6-well plates (a) and colony formation ratio (b) to demonstrate the effect of the nanoplatform on colony formation ability of MCF-7/ADR human breast cancer cells. The siRNA concentration in all groups was 150 pmol/mL. The DOX concentration in all groups was 1,000 ng/mL. *$P < 0.05$; **$P < 0.01$.

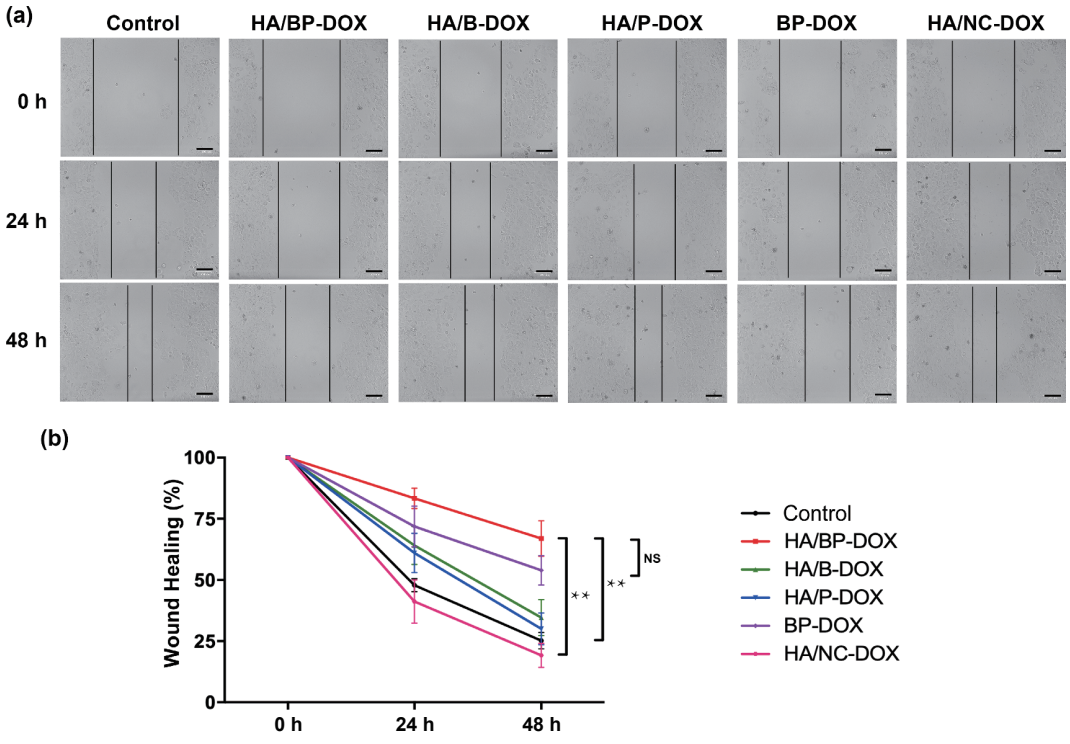

Figure 5 Effect of the complexes on wound healing ability of MCF-7/ADR human breast cancer cells (a, b). The siRNA concentration in all groups was 150 pmol/mL. The DOX concentration in all groups was 1,000 ng/mL. $^{*}P < 0.05$; $^{**}P < 0.01$. Scale bars: 100 μm.

3.4 *In vivo* antitumor effect of the polyplexes following intravenous injection

The advantages of targeted nanoplatform HA/BP with reversal of multidrug resistance breast cancer MCF-7/ADR cells by co-delivery of P-gp siRNA, Bcl-2 siRNA and DOX will potentially enhance the efficiency of antitumor effect *in vivo*. To demonstrate this, we examined the antitumor growth effect in mice with MCF-7/ADR xenografts by tail-vein injections of different formulations carrying DOX. There were five groups in the section. As illustrated in Fig. 6 and Fig. S5 in the ESM, treatment with the HA/NC-DOX, BP-DOX and DOX did not show tumor growth inhibition in comparison to the phosphate-buffered saline (PBS) group. However, co-delivery of DOX with P-gp siRNA and Bcl-2 siRNA by HA/BP-DOX to tumor-bearing mice showed a significant inhibition of tumor growth (73.26% inhibitory rate compared to the control group). It should be noted that the injection of siRNA carrying siNC did not inhibit tumor growth, indicating that reversal of multidrug resistance breast cancer MCF-7/ADR cells by P-gp siRNA and Bcl-2 siRNA was necessary for efficient drug

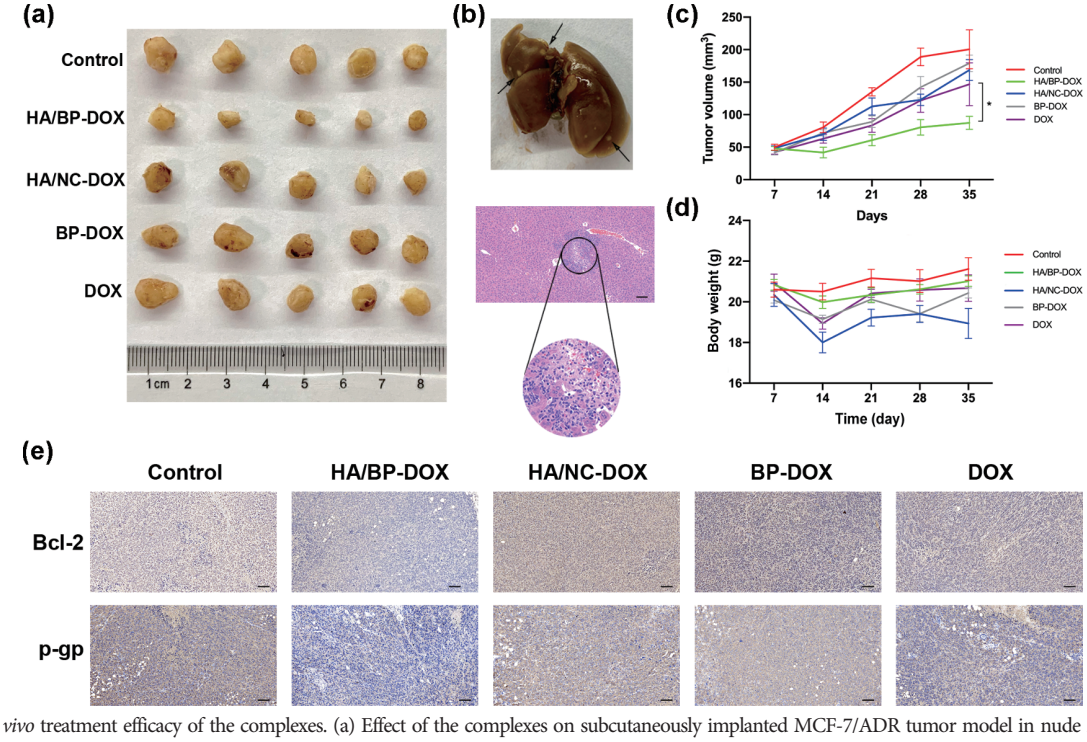

Figure 6 *In vivo* treatment efficacy of the complexes. (a) Effect of the complexes on subcutaneously implanted MCF-7/ADR tumor model in nude mouse. (b) The liver of mice treated with PBS has tumor metastasis. (c) The tumor volume of the HA/BP-DOX group was significantly decreased. (d) The weights of mouse remain the same. (e) Immunohistochemical analysis of Bcl-2 and p-gp protein expression in tumor tissues. $^{*}P < 0.05$. Scale bars: 100 μm.

delivery. Compared with HA/BP-DOX, BP-DOX polyplexes did not inhibit tumor growth, and this is mainly because hyaluronic acid enhanced the stability and the tumor targeting of the polyplexes *in vivo* [45]. It is worth mentioning that tumor liver metastasis was found in the liver of the mouse treated with PBS after the last injection (Fig. 6(b)).

The expression of P-gp and Bcl-2 protein in the tumor tissue after treatment was also analyzed by immunohistochemical analysis. As shown in Fig. 6(e), a decrease of P-gp and Bcl-2-positive tumoral cells (brown) in tumor tissue is shown upon treatment with HA/BP-DOX when compared with PBS treatment, which is corresponding to the results of inhibition of tumor growth. Hematoxylin and eosin (H&E) staining of major organs after the treatment indicated that no obvious toxicities were observed (Fig. 7).

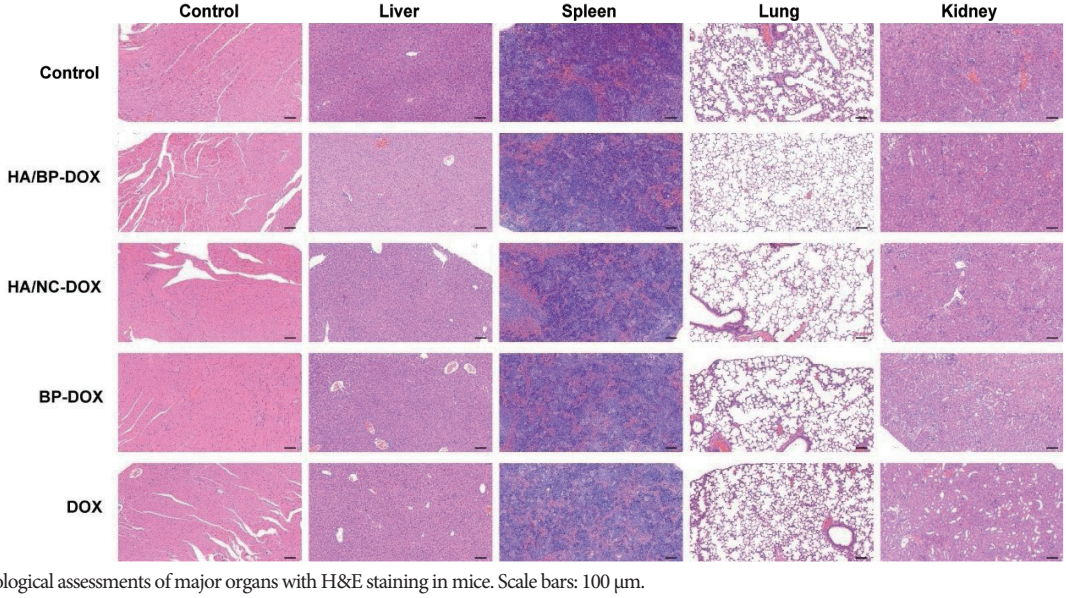

Figure 7 Histological assessments of major organs with H&E staining in mice. Scale bars: 100 μm.

4 Conclusions

We have developed a targeted nanoplatform with reversal of multidrug resistance breast cancer MCF-7/ADR cells by co-delivery of P-gp siRNA, Bcl-2 siRNA and DOX. HA/siP-gp-PLL-PBA9-siBcl-2-DOX complexes (HA/BP-DOX) with ATP-responsive nucleic acid release in cytoplasm and enhanced drug sensitivity exhibited a robust suppressing efficiency for the invasion, proliferation, and colony formation of MCF-7/ADR cells. In the *in vivo* antitumor experiment, HA/BP-DOX complexes showed significant inhibition of tumor growth with good biocompatibility. In summary, the nanoplatform established should provide biologists and engineers with a new tool to reverse multidrug resistance for efficient tumor treatment.

Acknowledgements

The authors take the grants from the National Natural Science Foundation of China (Nos. 81771968, 82003166, and 21704061), the Natural Science Foundation of Shanghai (No. 21ZR1439200), Shanghai Sailing Program (No. 17YF1411000), Shanghai Municipal Education Commission-Gaofeng Clinical Grant Support (No. 20181705), Shanghai Municipal Commission of Health and Family Planning (No. 201840020), and the Medical–Engineering Joint Funds from the Shanghai Jiao Tong University (Nos. ZH2018ZDA05 and YG2016QN54) on this work.

Electronic Supplementary Material: Supplementary material (^{1}H NMR spectra of the synthesized polymers in D_2O; cellular uptake of FAM-labelled siRNA delivered by PLL-PBA7 and PLL-PBA9 with N/P ratios of 1:1, 2:11, 4:1, 6:1, 8:1 and 10:1; DOX fluorescence of PLL-PBA9-siRNA/DOX/HA observed by fluorescence microscope with mass ratio range of PLL-PBA9 to HA from 1:0.5 to 1:3; ATP-responsive siRNA release of the nanoplatform) is available in the online version of this article at https://doi.org/10.1007/s12274-022-4254-1.

References

[1] DeSantis, C.; Siegel, R.; Bandi, P.; Jemal, A. Breast cancer statistics, 2011. *CA Cancer J. Clin.* **2011**, *61*, 409–418.
[2] Maughan, K. L.; Lutterbie, M. A.; Ham, P. S. Treatment of breast cancer. *Am. Fam. Physician* **2010**, *81*, 1339–1346.
[3] Wang, H.; Mao, X. Evaluation of the efficacy of neoadjuvant chemotherapy for breast cancer. *Drug Des. Devel. Ther.* **2020**, *14*, 2423–2433.
[4] Fisusi, F. A.; Akala, E. O. Drug combinations in breast cancer therapy. *Pharm. Nanotechnol.* **2019**, *7*, 3–23.
[5] Vaidya, J. S.; Massarut, S.; Vaidya, H. J.; Alexander, E. C.; Richards, T.; Caris, J. A.; Sirohi, B.; Tobias, J. S. Rethinking neoadjuvant chemotherapy for breast cancer. *BMJ* **2018**, *360*, j5913.
[6] Krug, D.; Loibl, S. Neoadjuvant chemotherapy for early breast cancer. *Lancet Oncol.* **2018**, *19*, e129.
[7] Cazzaniga, M. E.; Dionisio, M. R.; Riva, F. Metronomic chemotherapy for advanced breast cancer patients. *Cancer Lett.* **2017**, *400*, 252–258.
[8] Cazzaniga, M. E.; Pinotti, G.; Montagna, E.; Amoroso, D.; Berardi, R.; Butera, A.; Cagossi, K.; Cavanna, L.; Ciccarese, M.; Cinieri, S. et al. Metronomic chemotherapy for advanced breast cancer patients in the real world practice: Final results of the VICTOR-6 study. *Breast* **2019**, *48*, 7–16.
[9] Yuan, Y. L.; Cai, T. G.; Xia, X.; Zhang, R. H.; Chiba, P.; Cai, Y. Nanoparticle delivery of anticancer drugs overcomes multidrug resistance in breast cancer. *Drug Deliv.* **2016**, *23*, 3350–3357.
[10] Li, Y. L.; Gao, X. N.; Yu, Z. Z.; Liu, B.; Pan, W.; Li, N.; Tang, B. Reversing multidrug resistance by multiplexed gene silencing for enhanced breast cancer chemotherapy. *ACS Appl. Mater. Interfaces* **2018**, *10*, 15461–15466.
[11] Doyle, L. A.; Yang, W. D.; Abruzzo, L. V.; Krogmann, T.; Gao, Y. M.; Rishi, A. K.; Ross, D. D. A multidrug resistance transporter from human MCF-7 breast cancer cells. *Proc. Natl. Acad. Sci. USA* **1998**, *95*, 15665–15670.
[12] Chen, Z. L.; Shi, T. L.; Zhang, L.; Zhu, P. L.; Deng, M. Y.; Huang,

C.; Hu, T. T.; Jiang, L.; Li, J. Mammalian drug efflux transporters of the ATP binding cassette (ABC) family in multidrug resistance: A review of the past decade. *Cancer Lett.* **2016**, *370*, 153–164.

[13] Shi, X. L.; Dou, Y. H.; Zhou, K. R.; Huo, J. L.; Yang, T. J.; Qin, T. T.; Liu, W. H.; Wang, S. Q.; Yang, D. X.; Chang, L. M. et al. Targeting the Bcl-2 family and P-glycoprotein reverses paclitaxel resistance in human esophageal carcinoma cell line. *Biomed. Pharmacother.* **2017**, *90*, 897–905.

[14] Clarke, R.; Leonessa, F.; Trock, B. Multidrug resistance/P-glycoprotein and breast cancer: Review and meta-analysis. *Semin. Oncol.* **2005**, *32*, 9–15.

[15] Risnayanti, C.; Jang, Y. S.; Lee, J. J.; Ahn, H. J. PLGA nanoparticles co-delivering MDR1 and BCL2 siRNA for overcoming resistance of paclitaxel and cisplatin in recurrent or advanced ovarian cancer. *Sci. Rep.* **2018**, *8*, 7498.

[16] Wu, Y.; Zhang, Y.; Zhang, W.; Sun, C. L.; Wu, J. Z.; Tang, J. H. Reversing of multidrug resistance breast cancer by co-delivery of P-gp siRNA and doxorubicin via folic acid-modified core-shell nanomicelles. *Colloids Surf. B Biointerfaces* **2016**, *138*, 60–69.

[17] Mello, C. C.; Conte, D. Jr. Revealing the world of RNA interference. *Nature* **2004**, *431*, 338–342.

[18] Han, H. Y. RNA interference to knock down gene expression. *Methods Mol. Biol.* **2018**, *1706*, 293–302.

[19] Liu, H. M.; Wang, H.; Yang, W. J.; Cheng, Y. Y. Disulfide cross-linked low generation dendrimers with high gene transfection efficacy, low cytotoxicity, and low cost. *J. Am. Chem. Soc.* **2012**, *134*, 17680–17687.

[20] Shi, Y.; Lammers, T. Combining nanomedicine and immunotherapy. *Acc. Chem. Res.* **2019**, *52*, 1543–1554.

[21] Shen, W. W.; Wang, Q. W.; Shen, Y.; Gao, X.; Li, L.; Yan, Y.; Wang, H.; Cheng, Y. Y. Green tea catechin dramatically promotes RNAi mediated by low-molecular-weight polymers. *ACS Cent. Sci.* **2018**, *4*, 1326–1333.

[22] Yang, J. P.; Zhang, Q.; Chang, H.; Cheng, Y. Y. Surface-engineered dendrimers in gene delivery. *Chem. Rev.* **2015**, *115*, 5274–5300.

[23] Wang, H.; Huang, Q.; Chang, H.; Xiao, J. R.; Cheng, Y. Y. Stimuli-responsive dendrimers in drug delivery. *Biomater. Sci.* **2016**, *4*, 375–390.

[24] Lv, J.; Fan, Q. Q.; Wang, H.; Cheng, Y. Y. Polymers for cytosolic protein delivery. *Biomaterials* **2019**, *218*, 119358.

[25] Wang, M. M.; Liu, H. M.; Li, L.; Cheng, Y. Y. A fluorinated dendrimer achieves excellent gene transfection efficacy at extremely low nitrogen to phosphorus ratios. *Nat. Commun.* **2014**, *5*, 3053.

[26] Liu, H. M.; Wang, Y.; Wang, M. M.; Xiao, J. R.; Cheng, Y. Y. Fluorinated poly(propylenimine) dendrimers as gene vectors. *Biomaterials* **2014**, *35*, 5407–5413.

[27] Shi, C.; He, Y.; Feng, X. B.; Fu, D. H. ε-Polylysine and next-generation dendrigraft poly-L-lysine: Chemistry, activity, and applications in biopharmaceuticals. *J. Biomater. Sci. Polym. Ed.* **2015**, *26*, 1343–1356.

[28] Kim, S. W. Polylysine copolymers for gene delivery. *Cold Spring Harb Protoc.* **2012**, *2012*, 433–438.

[29] Chen, H. C.; Tian, J. W.; Liu, D. Y.; He, W. J.; Guo, Z. J. Dual aptamer modified dendrigraft poly-L-lysine nanoparticles for overcoming multi-drug resistance through mitochondrial targeting. *J. Mater. Chem. B* **2017**, *5*, 972–979.

[30] Kodama, Y.; Kuramoto, H.; Mieda, Y.; Muro, T.; Nakagawa, H.; Kurosaki, T.; Sakaguchi, M.; Nakamura, T.; Kitahara, T.; Sasaki, H. Application of biodegradable dendrigraft poly-L-lysine to a small interfering RNA delivery system. *J. Drug Target.* **2017**, *25*, 49–57.

[31] Kodama, Y.; Nakamura, T.; Kurosaki, T.; Egashira, K.; Mine, T.; Nakagawa, H.; Muro, T.; Kitahara, T.; Higuchi, N.; Sasaki, H. Biodegradable nanoparticles composed of dendrigraft poly-L-lysine for gene delivery. *Eur. J. Pharm. Biopharm.* **2014**, *87*, 472–479.

[32] Liu, Y.; Li, J. F.; Shao, K.; Huang, R. Q.; Ye, L. Y.; Lou, J. N.; Jiang, C. A leptin derived 30-amino-acid peptide modified pegylated poly-L-lysine dendrigraft for brain targeted gene delivery. *Biomaterials* **2010**, *31*, 5246–5257.

[33] Cottet, H.; Martin, M.; Papillaud, A.; Souaïd, E.; Collet, H.; Commeyras, A. Determination of dendrigraft poly-L-lysine diffusion coefficients by taylor dispersion analysis. *Biomacromolecules* **2007**, *8*, 3235–3243.

[34] Ryu, J. H.; Lee, G. J.; Shih, Y. R. V.; Kim, T. I.; Varghese, S. Phenylboronic acid-polymers for biomedical applications. *Curr. Med. Chem.* **2019**, *26*, 6797–6816.

[35] Winblade, N. D.; Nikolic, I. D.; Hoffman, A. S.; Hubbell, J. A. Blocking adhesion to cell and tissue surfaces by the chemisorption of a poly-L-lysine-*graft*-(poly(ethylene glycol); phenylboronic acid) copolymer. *Biomacromolecules* **2000**, *1*, 523–533.

[36] Peng, H. F.; Ning, X. Y.; Wei, G.; Wang, S. P.; Dai, G. L.; Ju, A. Q. The preparations of novel cellulose/phenylboronic acid composite intelligent bio-hydrogel and its glucose, pH-responsive behaviors. *Carbohydr. Polym.* **2018**, *195*, 349–355.

[37] Ye, L.; Liu, H. M.; Fei, X.; Ma, D.; He, X. Z.; Tang, Q. Y.; Zhao, X.; Zou, H. B.; Chen, X. J.; Kong, X. M. et al. Enhanced endosomal escape of dendrigraft poly-L-lysine polymers for the efficient gene therapy of breast cancer. *Nano Res.* **2021**, *15*, 1135–1144.

[38] Liu, C. Y.; Shao, N. M.; Wang, Y. T.; Cheng, Y. Y. Clustering small dendrimers into nanoaggregates for efficient DNA and siRNA delivery with minimal toxicity. *Adv. Healthc. Mater.* **2016**, *5*, 584–592.

[39] Liu, H. M.; Chang, H.; Lv, J.; Jiang, C.; Li, Z. X.; Wang, F.; Wang, H.; Wang, M. M.; Liu, C. Y.; Wang, X. Y. et al. Screening of efficient siRNA carriers in a library of surface-engineered dendrimers. *Sci. Rep.* **2016**, *6*, 25069.

[40] Liu, C. Y.; Wan, T.; Wang, H.; Zhang, S.; Ping, Y.; Cheng, Y. Y. A boronic acid-rich dendrimer with robust and unprecedented efficiency for cytosolic protein delivery and CRISPR-Cas9 gene editing. *Sci. Adv.* **2019**, *5*, eaaw8922.

[41] Abnous, K.; Danesh, N. M.; Ramezani, M.; Alibolandi, M.; Bahreyni, A.; Lavaee, P.; Moosavian, S. A.; Taghdisi, S. M. A smart ATP-responsive chemotherapy drug-free delivery system using a DNA nanostructure for synergistic treatment of breast cancer *in vitro* and *in vivo*. *J. Drug Target.* **2020**, *28*, 852–859.

[42] Ma, D.; Liu, H. M.; Zhao, P. P.; Ye, L.; Zou, H. B.; Zhao, X.; Dai, H. L.; Kong, X. M.; Liu, P. F. Programing assembling/releasing multifunctional miRNA nanomedicine to treat prostate cancer. *ACS Appl. Mater. Interfaces* **2020**, *12*, 9032–9040.

[43] Friedl, P.; Alexander, S. Cancer invasion and the microenvironment: Plasticity and reciprocity. *Cell* **2011**, *147*, 992–1009.

[44] Paul, C. D.; Mistriotis, P.; Konstantopoulos, K. Cancer cell motility: Lessons from migration in confined spaces. *Nat. Rev. Cancer* **2017**, *17*, 131–140.

[45] Mattheolabakis, G.; Milane, L.; Singh, A.; Amiji, M. M. Hyaluronic acid targeting of CD44 for cancer therapy: From receptor biology to nanomedicine. *J. Drug Target.* **2015**, *23*, 605–618.